
The World is Not Mono: Enabling Spatial Understanding in Large Audio-Language Models

Yuhuan You¹ Lai Wei¹ Xihong Wu¹ Tianshu Qu¹

Abstract

Existing large audio-language models perceive the world as "mono"—a single stream of audio that ignores the critical spatial dimension ("where") required for universal audio scene analysis (ASA). To bridge this gap, we first introduce a hierarchical framework for audio scene analysis. Guided by this framework, we introduce a system that enables large audio-language models (LALMs) to understand and reason about the complex acoustic world. Our system endows LALMs with universal spatial understanding through four key innovations: (1) A scalable simulation pipeline that synthesizes high-quality First-Order-Ambisonics(FOA) data; (2) A unified model framework that integrates universal spatial encoding with a dense hybrid projection mechanism to bridge the modality gap; (3) A progressive training curriculum that evolves from representation alignment to reinforcement learning-based reasoning; and (4) A comprehensive benchmark for audio scene analysis (ASA) designed to rigorously evaluate atomic perception, relational integration, and cognitive reasoning capabilities, on which our model demonstrates comparatively strong capability for spatial understanding. Our work provides a clear pathway for leveraging the powerful reasoning abilities of LALMs towards holistic ASA, advancing from "mono" semantic recognition to spatial intelligence.

1. Introduction

The transition of Large Language Models (LLMs) to multimodal intelligence has spurred interest in the auditory domain. While recent Large Audio-Language Models (LALMs) demonstrate strong semantic understanding ('what') (Chu et al., 2024; Yang et al., 2024), they pre-

¹School of Intelligence Science and Technology, Peking University, Beijing, China. Correspondence to: Tianshu Qu <qtianshu@pku.edu.cn>.

Preprint. February 5, 2026.

dominantly treat audio as monophonic, neglecting spatial attributes ('where'). This lack of spatial reasoning contrasts with biological hearing, where binaural cues are essential for source localization and stream segregation (the 'cocktail party effect'). Although recent works have explored spatial encoding via First-Order Ambisonics (FOA) (You et al., 2025; Zheng et al., 2025), approaches remain fractured between semantic understanding (Tang et al., 2024) and physical parameter estimation (Shimada et al., 2021).

To systematically bridge this gap, we introduce a three-layer cognitive framework for Auditory Scene Analysis (ASA), inspired by Bregman's perceptual theory (Bregman, 1990):

- **L1: Atomic Perception:** Identifying discrete properties (semantic class and spatial location).
- **L2: Relational Integration:** Binding disparate attributes into coherent auditory objects (e.g., associating a specific sound with a specific location).
- **L3: Cognitive Reasoning:** Inferring complex relationships and causality using world knowledge.

Current LALMs fail to satisfy the spatial requirements of these levels. Addressing the scarcity of spatial data in standard datasets (Fonseca et al., 2022; Drossos et al., 2019a; Shimada et al., 2023), we leverage physically-consistent simulation (Scheibler et al., 2017) to generate large-scale training corpora.

We propose **The World is Not Mono (TWNM)**, a framework extending LALMs to spatial reasoning through high-fidelity FOA simulation and a unified architecture. Our main contributions are:

1. **Scalable FOA Simulation Pipeline:** We construct a pipeline simulating diverse room acoustics and trajectories to provide physically grounded spatial cues.
2. **Unified Model Framework:** We integrate a slot-based spatial encoder with a dense hybrid projection strategy to bridge the modality gap.
3. **Progressive Training Curriculum:** We employ a curriculum evolving from representation alignment to

Soft Adaptive Policy Optimization (SAPO) (Gao et al., 2025), aligning reasoning with physical evidence.

4. **Comprehensive ASA Benchmark:** We establish a benchmark to strictly evaluate atomic perception, relational integration, and cognitive reasoning capabilities.

The paper is organized as follows: Section 2 reviews related work; Section 3 formulates the ASA task; Section 4 details the architecture and training; Section 5 presents experiments; and Section 6 concludes.

2. Related Work

Audio–Language Foundation Models and Evaluation.

Recent large audio–language models (LALMs) connect an audio encoder to an LLM to enable instruction following and open-ended reasoning over speech, environmental sounds, and music (Chu et al., 2024; Tang et al., 2024; Huang et al., 2023). Despite strong progress on semantic understanding (the “what”), most public pipelines still treat audio as a monophonic time series and rarely evaluate explicit spatial perception or spatial reasoning (the “where”) (Yang et al., 2024). As a result, current LALMs remain poorly characterized—and often under-trained—for direction, distance, and cross-source spatial relations.

Spatial Audio with LLM Interfaces. A small but growing body of work extends the encoder-to-LLM paradigm to spatial audio. BAT introduces spatial question answering over binaural/spatial mixtures and reports promising results on benchmark-style QA (Zheng et al., 2025). ELSA explores aligning spatial audio and text representations via contrastive objectives to support retrieval/localization in an open-vocabulary form (Devnani et al., 2024). However, existing approaches still leave open questions on representation choice (binaural vs. FOA), multi-source correspondence (binding), and training strategies that ground language outputs in physical acoustic evidence.

Computational Audio Scene Analysis and 3D SELD.

Spatial hearing has long been studied in computational ASA/SELD, where systems predict sound classes and directions from multichannel audio (often FOA) (Shimada et al., 2021; 2023). These methods are effective for structured outputs and closed-set taxonomies, but they do not naturally support conversational querying, open-vocabulary descriptions, or multi-step reasoning—capabilities central to LALMs.

Data Synthesis for Spatial Supervision. Large-scale corpora with joint semantic labels and reliable 3D geometry/trajectory annotations are scarce. Consequently, many spatial pipelines rely on physically grounded simulation, combining non-spatial content collections (Fonseca et al., 2022;

Drossos et al., 2019a; Agostinelli et al., 2023) with room acoustics toolkits (Scheibler et al., 2017) to generate reproducible spatial training and evaluation data.

Architectures and Alignment Paradigms. Scaling recipes from LLMs motivate modular specialization (e.g., sparse MoE) (Fedus et al., 2022; Lepikhin et al., 2020), while modern post-training methods (e.g., group-based policy optimization) can improve reasoning reliability and output format compliance (Shao et al., 2024). Applying such alignment to spatial audio remains early-stage, especially when the objective must penalize hallucinations and reward answers that are consistent with acoustic spatial cues.

3. Task Definition of Audio Scene Analysis

We formally define the Audio Scene Analysis (ASA) task by deconstructing it into a three-layer cognitive framework: Atomic Perception (\mathcal{L}_1), Relational Integration (\mathcal{L}_2), and Cognitive Reasoning (\mathcal{L}_3). This hierarchical formulation aligns with classical ASA theories—moving from raw sensory signals to structured conceptual understanding—and provides a rigorous mathematical basis for evaluating machine auditory systems.

3.1. Preliminaries and Definitions

We define an auditory scene \mathcal{S} as a composition of atomic units governed by physical acoustic laws and semantic rules. The system input is a multi-channel audio waveform $\mathbf{X} \in \mathbb{R}^{C \times L}$, where C is the number of channels and L is the sequence length.

Auditory Objects (\mathcal{O}): Let $\mathcal{O} = \{o_1, \dots, o_N\}$ denote the set of perceived auditory objects. We define each object o_i as a disentangled attribute tuple:

$$o_i = (c_i, \mathbf{s}_i) \quad (1)$$

where $c_i \in \mathcal{C}$ denotes the **semantic class** label from a pre-defined vocabulary \mathcal{C} (covering both foreground events and background environments). $\mathbf{s}_i \in \mathbb{R}^3$ denotes the **spatial coordinate vector** (e.g., azimuth, elevation, and distance) relative to the listener.

Note on Temporal Scope: A complete event definition typically includes a temporal span $\tau_i = [t_{\text{start}}, t_{\text{end}}]$. While the temporal dimension is a fundamental pillar of ASA, this specific task definition emphasizes the integration of semantic and spatial dimensions within a coherent observation window.

Knowledge Base (\mathcal{K}): We assume access to a global knowledge base \mathcal{K} , which encodes physical laws (e.g.,

sound propagation), schemas (e.g., typical environment-sound pairs), and causal priors required for high-level reasoning.

3.2. Layer 1: Atomic Perception (\mathcal{L}_1)

The foundational layer \mathcal{L}_1 focuses on the extraction of discrete, statistically independent attributes from the raw waveform \mathbf{X} . At this stage, the task is to act as a mapping function $f_{\mathcal{L}_1}$ that identifies “what” and “where” without yet inferring high-order dependencies between detections.

Formally, \mathcal{L}_1 produces a set of candidate detections $\hat{\mathcal{O}}$:

$$\hat{\mathcal{O}} = f_{\mathcal{L}_1}(\mathbf{X}) = \{(\hat{c}_i, \hat{s}_i)\}_{i=1}^N \quad (2)$$

This layer operates on two parallel dimensions: semantic Classification tasks estimate the categorical identity \hat{c}_i , while spatial localization tasks estimate the physical coordinates \hat{s}_i . The goal of atomic perception is to translate continuous acoustic energy into a symbolic list of potential entities, though these attributes are initially treated as isolated observations.

3.3. Layer 2: Relational Integration (\mathcal{L}_2)

The second layer \mathcal{L}_2 moves beyond isolated detections to perform Scene Graph Construction. It transforms the unstructured set $\hat{\mathcal{O}}$ into a structured graph $\mathcal{G} = (\mathcal{V}, \mathcal{E})$, where nodes \mathcal{V} correspond to validated objects and edges \mathcal{E} represent their mutual relationships.

Intra-Object Binding (Object Validation): This process addresses the “binding problem”—verifying if a semantic attribute c and a spatial attribute s belong to the same physical entity. We formulate this as a conditional probability estimation: given a subset of observed attributes $\mathbf{a} \subset \{c, \mathbf{s}\}$, the task is to infer the complementary attributes $\bar{\mathbf{a}}$:

$$\hat{\bar{\mathbf{a}}} = \operatorname{argmax}_{\bar{\mathbf{a}}} P(\bar{\mathbf{a}} \mid \mathbf{a}, \mathbf{X}) \quad (3)$$

This enables cross-modal inference, such as deducing location from semantics ($c \rightarrow s$) or identifying a source via its spatial trajectory.

Inter-Object Relations (Edge Formation): Edges $\mathcal{E} = \{r_{ij} \mid i \neq j\}$ capture interactions between objects via a relational operator Φ :

$$r_{ij} = \Phi(o_i, o_j) \quad (4)$$

These relations include spatial-physical interactions (e.g., masking) and spectral-temporal dependencies (e.g., harmonic compatibility).

3.4. Layer 3: Cognitive Reasoning (\mathcal{L}_3)

The apex layer \mathcal{L}_3 executes probabilistic inference over the scene graph \mathcal{G} and the knowledge base \mathcal{K} , representing the transition from “hearing” to “understanding.” The process is modeled as:

$$Y^* = \operatorname{argmax}_Y P(Y \mid \mathcal{G}, \mathcal{K}) \quad (5)$$

where Y is a high-level judgment. \mathcal{L}_3 facilitates advanced reasoning tasks:

1. **Abductive & Causal Inference:** Distinguishes correlation from causality (e.g., sequential impacts) and infers global context from local evidence (e.g., vehicle sounds \rightarrow “traffic”).
2. **Deductive & Commonsense Validation:** Validates perception using physical constraints (e.g., material properties from impact) and detects semantic anomalies via environmental priors.
3. **Inductive & Analogical Generalization:** Generalizes recurring structures (e.g., alternating vocals \rightarrow “dialogue”) and characterizes unknown sources via physical analogy (e.g., Doppler \rightarrow motion).
4. **Multi-hop Traversal & Metacognition:** Executes graph traversal for complex queries (e.g., temporal search) and performs metacognitive tasks like counterfactual reasoning (e.g., no response \rightarrow “empty”).

4. Methodology

4.1. Preliminaries: First-Order Ambisonics

Ambisonics represents a sound field by decomposing the sound pressure $p(k, \mathbf{r})$ into spherical harmonics $Y_n^m(\theta, \phi)$ (Rafaely, 2015):

$$p(k, r, \theta, \phi) = 4\pi \sum_{n=0}^{\infty} \sum_{m=-n}^n i^n j_n(kr) B_n^m Y_n^m(\theta, \phi) \quad (6)$$

where B_n^m are the Ambisonics coefficients encoding the spatial information.

In this work, we focus on First-Order Ambisonics (FOA), which truncates the expansion at $n = 1$. This yields a 4-channel B-format signal $\mathbf{x}(t) = [W(t), Y(t), Z(t), X(t)]^T$. Here, W is the zero-th order omnidirectional pressure, while $\{X, Y, Z\}$ are the first-order pressure gradients (dipoles) along the Cartesian axes. This compact representation provides the essential 3D cues—azimuth, elevation, and distance—required for spatial reasoning within our model.

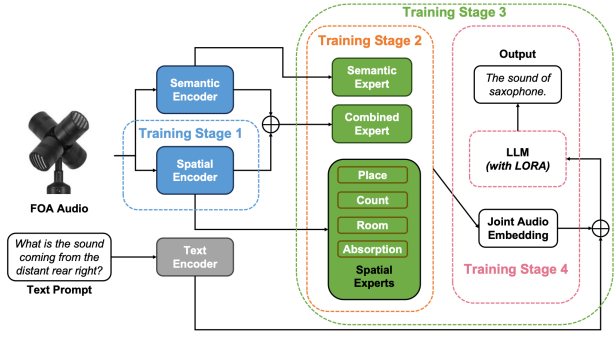


Figure 1. TWNM Model Architecture.

4.2. Model Architecture

The TWNM framework employs a dual-branch architecture to reconcile semantic audio understanding with spatial scene analysis. The system consists of two parallel processing streams: a *semantic branch* and a *spatial branch*. The semantic branch utilizes a pre-trained large audio-language backbone to extract high-level linguistic and event-related features from omnidirectional audio. Simultaneously, the spatial branch processes First-Order Ambisonics (FOA) input to resolve the 3D physical geometry of the acoustic scene. Features from both branches are aligned through a projection layer and interleaved into a multimodal sequence, which is then fed into the language model for spatial understanding.

4.2.1. HIERARCHICAL SPATIAL ENCODER

The spatial encoder \mathcal{E}_{spat} is architected to map 4-channel First-Order Ambisonics (FOA) waveforms $\mathbf{x} \in \mathbb{R}^{4 \times L}$ to a structured set of physical primitives. The internal topology consists of a stack of 8 layer blocks, organized into three functional stages: grouped spectral projection, spatio-temporal modeling, and recursive object discovery.

Grouped Spectral Projection The input waveform is transformed into the frequency domain via a Short-Time Fourier Transform (STFT) using a window size of 256 points and a hop size of 128 points. To retain complete phase information crucial for localization, the complex-valued coefficients are unrolled into an 8-channel real-valued spectro-temporal map $\mathbf{X} \in \mathbb{R}^{8 \times F \times T}$, where $F = 129$ represents the single-sided frequency bins. The initial projection employs a 1D convolution with a kernel size of 5 and a hidden dimension of 96. To preserve spatial gradients across FOA channels, features are processed in 4 independent spatial groups using Group BatchNorm (GBN) to ensure directional intensity information is preserved before high-level abstraction.

Spatio-Temporal Modeling The core modeling involves a tripartite sequence within each layer: (1) *cross-band* modeling using grouped frequency convolutions (kernel size 5, 8 groups); (2) *full-band* global interaction via a linear interaction module that reduces frequency channels to a bottleneck dimension of 8 before projection; and (3) *narrow-band* temporal modeling using Multi-Head Self-Attention (MHSA) and temporal convolutions with a feed-forward expansion dimension of 192.

Attractor-based Object Discovery To resolve discrete auditory objects from the temporal feature map, we utilize a recursive attractor module implemented with an LSTM. This module iteratively generates $K = 3$ discrete object slots. These slots serve as dynamic queries for a cross-attention layer to extract object-specific features \mathbf{h}_i^{slot} from the encoder output. For each slot, the module predicts an existence probability $p_i \in [0, 1]$ to facilitate source counting and detection.

Multi-Task Output Heads The slot embeddings are passed through parallel heads: unit direction vectors $\mathbf{u}_i \in \mathbb{S}^2$ (normalized via L_2 norm), radial distances $d_i \in \mathbb{R}^+$ (constrained by a Softplus activation), and semantic classes. Additionally, a global scene token estimates the room surface area A_{room} and the average absorption coefficient $\bar{\alpha} \in [0, 1]$. A learnable gating mechanism partitions the final 192-dimensional pooled representation into specialized spatial and semantic sub-components for downstream fusion.

4.2.2. HYBRID FEATURE PROJECTION

The projector maps the decoupled semantic and spatial embeddings into the input space of the Large Language Model (LLM). We employ a *Dense Hybrid* architecture (P2 mode) to ensure that explicit spatial physics and implicit semantic contexts are concurrently preserved.

Expert Pathways Let $\mathbf{H}_{sem} \in \mathbb{R}^{T \times 768}$ and $\mathbf{H}_{spat} \in \mathbb{R}^{T \times 768}$ be the 768-dimensional outputs from the semantic (Whisper) and spatial encoders, respectively. The projection module activates all specialized pathways for every token:

- **Semantic Expert:** A Feed-Forward Network (FFN) aligns linguistic and general audio representations.
- **Spatial Experts:** A set of $N = 4$ parallel FFNs specialized for key acoustic dimensions: source coordinates (direction and distance), room geometry, absorption characteristics, and source count.
- **Combined Expert:** An FFN processes the element-wise sum ($\mathbf{H}_{sem} + \mathbf{H}_{spat}$) to explicitly model the latent interactions between semantic content and spatial context.

Bottleneck Fusion To maintain efficiency and adhere to parameter-matching constraints, the outputs from all experts are concatenated and projected to the LLM’s hidden dimension D_{LLM} through a bottleneck MLP block:

$$\begin{aligned} \mathbf{O}_{sp} &= \text{Concat}_{k=1}^4 [\mathcal{E}_{sp}^k(\mathbf{H}_{spat})] \\ \mathbf{H}_{cat} &= \text{Concat} [\mathcal{E}_{sem}(\mathbf{H}_{sem}), \mathbf{O}_{sp}, \mathcal{E}_{comb}(\mathbf{H}_{sem} + \mathbf{H}_{spat})] \\ \mathbf{E}_{audio} &= \mathbf{W}_2 \cdot \text{GELU}(\mathbf{W}_1 \cdot \text{LN}(\mathbf{H}_{cat})) \end{aligned} \quad (7)$$

where LN denotes Layer Normalization. \mathbf{W}_1 projects the high-dimensional concatenated vector to a smaller bottleneck dimension to stabilize the cross-modal interface, while \mathbf{W}_2 performs the final alignment to the latent space of the LLM decoder.

4.2.3. BACKBONE INTEGRATION AND MULTIMODAL ALIGNMENT

The integration between the multimodal encoders and the LLM decoder is achieved through sequence-level embedding concatenation, adhering to the architectural paradigms of Audio Flamingo (Goel et al., 2025). This section delineates the mechanism by which projected audio representations are interleaved with linguistic tokens to facilitate joint spatio-temporal and semantic reasoning.

Audio-Text Sequence Construction The input to the LLM decoder is structured as a unified sequence of continuous embeddings. During inference and training, the text prompt is tokenized, and the specific insertion point for auditory information is identified by a reserved anchor token, `<AcousticTokens>`. The continuous audio embeddings $\mathbf{E}_{audio} \in \mathbb{R}^{T_{audio} \times D_{LLM}}$ generated by the hybrid projector are directly substituted into the sequence at the anchor’s position:

$$\mathbf{H}_{in} = [\mathbf{E}_{prefix}, \mathbf{E}_{audio}, \mathbf{E}_{suffix}] \quad (8)$$

where \mathbf{E}_{prefix} and \mathbf{E}_{suffix} represent the frozen linguistic embeddings from the LLM vocabulary. Since the hybrid projector aligns the audio features with the decoder’s hidden dimension $D_{LLM} = 4096$ (optimized for the Qwen2-7B backbone), the decoder processes \mathbf{E}_{audio} as a sequence of high-dimensional "soft tokens" without requiring modifications to the underlying Transformer blocks.

Training Objective and Parameter Initialization The decoder’s parameters are initialized from the Flamingo3 pre-trained model to leverage its robust multimodal prior. To adapt the model to spatial reasoning while preserving its generative fluency, we employ an *answer-only causal language modeling* objective. The negative log-likelihood loss is computed exclusively over the response tokens, while prompt and audio token positions are assigned a label of

−100 to be ignored during gradient calculation:

$$\mathcal{L} = - \sum_{i=1}^N \log P(y_i | y_{<i}, \mathbf{E}_{audio}, \mathbf{E}_{prompt}) \quad (9)$$

This strategy ensures that the optimization pressure is focused on refining the cross-modal alignment between the decoupled spatial experts and the linguistic decoder.

Unified Attention Mechanism Within the decoder, we maintain a standard causal self-attention framework, eschewing additional cross-attention layers to minimize structural overhead. Spatial representations from \mathcal{E}_{spat} and semantic features from \mathcal{E}_{sem} are projected into the same latent space, allowing the model to perform holistic reasoning by cross-referencing physical evidence (e.g., source distance or direction) with the semantic attributes of the auditory objects within a single attention pass.

4.3. Learning: A Progressive Curriculum from Representation to Policy

To explicitly bridge the gap between physical acoustic perception and cognitive reasoning, we implement a rigorous four-stage curriculum: Representation → Alignment → SFT → Policy.

Stage 1: Representation Learning. We pre-train the spatial encoder \mathcal{E}_{spat} using a **two-phase strategy** to ensure both physical consistency and real-world robustness.

- *Phase I (Synthetic Warm-up):* The encoder is first trained exclusively on a large-scale synthetic dataset. This allows the model to learn fundamental acoustic physics using perfect ground-truth labels for direction, distance, and reverberation.
- *Phase II (Sim-to-Real Adaptation):* We then fine-tune the model on a mixed corpus comprising 70% simulation and 30% real-world recordings. For real-world samples, we mask out noisy semantic and environmental losses, enforcing supervision only on high-confidence spatial localization tasks (direction and distance). This prevents the encoder from overfitting to label noise inherent in real data while adapting to realistic recording conditions.

Stage 2: Projector Alignment (Alignment I). We freeze both the encoders and the LLM backbone, training only the dense hybrid projector. This module features a specialized combined expert pathway that processes the element-wise sum of semantic and spatial features ($\mathbf{H}_{sem} + \mathbf{H}_{spat}$). By densely concatenating the outputs of semantic, spatial, and combined experts, the projector explicitly captures early cross-modal interactions before mapping them to the LLM’s embedding space.

Stage 3: Supervised Fine-Tuning (SFT). This stage unifies instruction following and Chain-of-Thought (CoT) formatting. We jointly train the projector and the LLM’s LoRA adapters. We employ a *reasoning-and-answer-only* loss mask, ensuring that gradients are back-propagated solely from the generated reasoning steps and the final answer, while the instruction prompt and the inserted `<AcousticTokens>` anchor remain masked.

Stage 4: Policy Optimization via SAPO. We treat the SFT model as a policy π_θ and align it using SAPO (Gao et al., 2025). Unlike standard GRPO, SAPO utilizes a sigmoid-smoothed loss function to stabilize policy updates against high-variance advantages. Settings are detailed in Appendix B.

5. Experiments

This section details the experimental evaluation of our framework.

5.1. Datasets and Simulation Pipeline

To support the progressive training of TWNM, we constructed a comprehensive data pipeline encompassing large-scale synthesis, sim-to-real adaptation, and a structured evaluation benchmark.

Synthetic FOA Corpus. We developed a scalable simulation pipeline to generate high-quality First-Order Ambisonics (FOA) data.

Source Materials: We sampled dry audio from three distinct domains to cover diverse semantic hierarchies: environmental sounds from Clotho (Drossos et al., 2019b), speech from LibriTTS-R (Koizumi et al., 2023), and music from SongDescriber (Manco et al., 2023), mixed with a ratio of 5:3:2.

Acoustic Simulation: We utilized Pyroomacoustics to simulate Shoebox rooms with explicit acoustic modeling. Rooms were categorized into Small (3–5m), Medium (5–8m), and Large (8–15m) with sampling probabilities of 0.6, 0.3, and 0.1, respectively. Absorption coefficients were sampled from Dry (0.7–0.99), Moderate (0.3–0.7), and Wet (0.1–0.3) ranges to vary reverberation times (RT_{60}).

Spatial Configuration: A virtual 4-channel FOA microphone array was placed at a height of 1.7m. For each sample, up to 3 sound sources were placed with random azimuths (0–360°), elevations (−90–90°), and valid distances (> 0.5m from boundaries). We generated 50k samples for this phase.

Sim-to-Real Adaptation. To bridge the domain gap, we fine-tuned the spatial encoder on a mixed corpus comprising the synthetic data and real-world recordings from the

STARSS23 dataset (Shimada et al., 2023).

Mixing Strategy: We employed a deterministic mixing ratio of 7:3 (Sim:Real). To address the label imbalance in real-world data, we applied a re-balancing strategy that over-samples real data based on the number of active sources (k).

Domain-Adaptive Supervision: Recognizing that real-world data lacks reliable ground truth for room acoustics and precise semantic labels aligned with our vocabulary, we implemented a masked loss mechanism. For real-world samples, we masked the gradients for semantic classification and room parameter estimation enforcing supervision solely on robust spatial tasks: direction, distance, and source counting.

5.2. Benchmark Construction

To rigorously evaluate the hierarchical spatial reasoning capabilities of LALMs, we construct a comprehensive benchmark comprising 1,000 multiple-choice questions (MCQs). Unlike existing benchmarks that primarily focus on semantic recognition, our benchmark is structurally aligned with the proposed three-layer ASA framework.

5.2.1. DATA GENERATION PIPELINE

Since manual annotation of spatial attributes (e.g., exact distance, coordinates) is error-prone and unscalable, we employ a simulation-based generation pipeline to ensure ground-truth correctness.

Rich Text Scene Description (RTSD). For every synthesized audio mixture in the test set, we programmatically generate a hidden RTS. This text contains the absolute ground truth of the scene, including source classes, precise coordinates (r, θ, ϕ), room dimensions, and reverberation parameters.

Prompt-Driven QA Generation. We design a set of self-contained prompts for a teacher LLM. Each prompt takes the RTS as input and outputs a strict JSON object containing the question, four options, and the correct answer. Crucially, the RTS is hidden from the student model during evaluation to prevent information leakage.

5.2.2. TASK TAXONOMY AND DISTRIBUTION

The benchmark is stratified into three cognitive levels. A detailed breakdown of task families and example questions is provided in Table 5.

Level 1: Static Identification (32.1%). This layer evaluates the model’s ability to perceive atomic attributes of individual sound sources. It serves as the sensory founda-

tion, covering fundamental competencies such as numeracy, semantic classification, and absolute spatial localization.

Level 2: Relational Integration (28.5%). This layer assesses the model’s capacity to “bind” disparate attributes (e.g., content + location) into coherent objects and quantify relationships between them. It focuses on cross-modal verification, retrieval, and spatial comparisons.

Level 3: Cognitive Reasoning (39.4%). The apex layer tests the model’s ability to perform logical inference using acoustic evidence and physical constraints. This includes complex tasks such as abductive reasoning (inferring scene context), counterfactual simulation (e.g., observer rotation), and multi-hop logical deduction.

5.3. Diagnostic Analysis: Spatial Encoder Robustness

Before evaluating the end-to-end LALM, we rigorously validate the robustness of our foundational Spatial Encoder (Stage 1). We benchmark our approach against established signal processing and deep learning baselines using both synthetic metrics and the real-world STARSS23 (Shimada et al., 2023) dataset.

Reference Performance in Simulation. First, to establish the theoretical capability of the encoder architecture, we report performance on standard synthetic benchmarks (Table 1).

- **EINV2** (Hu et al., 2022): A signal processing baseline. It achieves moderate counting accuracy (66.4%) but struggles with precise localization.
- **Sp-ACCDOA** (Shimada et al., 2022): A state-of-the-art deep learning baseline. While it achieves strong results (87.3% count acc), our proposed **TWNM Encoder** outperforms it across all metrics, achieving **89.4%** counting accuracy and reducing localization error to **7.9°**.

This confirms that our disentangled Attractor-based architecture provides a superior representation foundation in ideal conditions.

The Reality Gap and Domain Adaptation. However, high performance in simulation does not guarantee real-world utility. Table 2 presents the evaluation on the real-world STARSS23 dataset.

- **Sim-Only Failure:** When trained solely on simulation, even our strong encoder suffers from severe domain shift (*Acc* drops to 30.6%).

Table 1. Reference Performance on Synthetic Data. Comparison of our encoder against baselines in a pure simulation setting. Our model achieves superior precision in both counting and localization. Baseline data sourced from (Du et al., 2026).

Method	Count Acc	Loc. Error (°)	Dist. Error (m)
EINV2	66.4	86.1 [†]	2.47
Sp-ACCDOA	87.3	21.8 [†]	1.01
Ours	89.4	7.9	0.27

[†] Reported as Azimuth Error (ϵ_{azi}). Ours is Mean Angular Error.

Table 2. Real-World Adaptation on STARSS23. Models trained without real-world adaptation (Sim-Only) degrade significantly. Our Sim-to-Real strategy recovers performance, surpassing the DCASE baseline.

Method	DOA (°)	Dist (m)	Detection
<i>Baselines (Real-World)</i>			
TWNM (Sim-Only)	25.7	0.48	30.6% (Acc)
DCASE24 Base [‡]	29.6	0.31 [§]	18.0% (F ₂₀)
<i>Ours (Adapted)</i>			
TWNM (Sim-to-Real)	22.5	0.38	81.7% (Acc)

[‡] Evaluated on DCASE24 Task 3 Track A (Audio-Only).

[§] Relative distance error (unitless).

- **Sim-to-Real Success:** By applying our 7:3 Sim-to-Real mixing strategy, we bridge this gap. Our adapted encoder achieves a counting accuracy of **81.7%** and a DOA error of **22.5°**, significantly outperforming the DCASE 2024 audio-only baseline (29.6°).

This contrast highlights that while architectural innovations (Table 1) are necessary for precision, *data-centric domain adaptation* (Table 2) is decisive for real-world robustness.

Scope of Sim-to-Real Evaluation. It is important to clarify that our Sim-to-Real evaluation is strictly confined to the Stage 1 Spatial Encoder. Manually annotating high-fidelity spatial reasoning chains for real-world recordings is prohibitively time-consuming. Furthermore, we found that prompting LLMs to generate QA pairs based on complex, frame-wise RTSDs of real-world data often leads to severe *modality mismatches* and *hallucinations*. Consequently, we focus our real-world validation on the physical perception layer (Stage 1) to ensure rigor.

5.4. Main Results

To contextualize the performance of TWNM, we compare it against BAT (Zheng et al., 2025), a representative state-of-the-art baseline. Since BAT lacks the capability to generate structured chain-of-thought outputs, we adopted a hybrid evaluation protocol. For \mathcal{L}_1 Perception, we evaluated BAT using direct generation. For complex \mathcal{L}_2 Integration and \mathcal{L}_3 Reasoning tasks, we converted the multi-choice questions

Table 3. Main Experiment and ablation of model capabilities across training stages. We compare our progressive checkpoints against the baseline.

Model / Stage	ASA Competency Levels			Overall
	\mathcal{L}_1	\mathcal{L}_2	\mathcal{L}_3	
BAT	24.68 [†]	31.39 [†]	29.89 [†]	28.30
Align	53.25	29.39	43.15	43.20
SFT	65.19	70.61	51.19	62.00
SAPO	63.64	69.89	79.76	70.80

[†]Measured as Per-Option Accuracy (Binary T/F, random=50%); others are standard MCQA (random=25%).

into boolean (True/False) discrimination tasks for each option and report the “Per-Option Accuracy”. Note that for this binary metric, a random guess yields 50%, whereas standard MCQA accuracy for our model has a random baseline of 25%.

As shown in Table 3, the baseline BAT achieves only 29.89% on \mathcal{L}_3 tasks—significantly below the random chance threshold of 50%. This indicates that without explicitly decoupled spatial representations, generic LALMs suffer from systematic hallucinations when faced with spatial queries. In contrast, our model, equipped with the Hybrid Feature Projector and optimized via SAPO, achieves robust performance (79.76%) on the stricter MCQA metric, validating the necessity of our architecture for high-level reasoning.

Our curriculum constitutes a staged ablation where each phase contributes a distinct capability. Moving from base feature alignment (Stage 2) to instruction tuning (Stage 3) and finally to policy optimization (Stage 4), overall accuracy consistently rises from 43.20% to 70.80%.

The Emergence of Attribute Binding (\mathcal{L}_2). A critical observation is the sharp performance jump in \mathcal{L}_2 Integration tasks between Stage 2 (29.39%) and Stage 3 (70.61%). While Stage 2 successfully aligns atomic features (achieving 53.25% on \mathcal{L}_1), it fails to “bind” them into coherent objects. This suggests that the mechanism of binding—associating a specific sound *content* with a specific *location*—is not merely a perceptual alignment task but a logic-driven process that requires the Chain-of-Thought capabilities unlocked during Stage 3 SFT.

SAPO Unlocks Cognitive Reasoning (\mathcal{L}_3). Consistent with our hypothesis, Stage 4 (SAPO) yields the most dramatic gains in complex reasoning. While Stage 3 improves general instruction following, it struggles with abstract tasks like *Physical Consistency* and *Scene Abduction*. SAPO boosts \mathcal{L}_3 accuracy from 51.19% to 79.76%. Specifically,

performance on *Scene Abduction* surges from 37.5% to 87.5%, confirming that preference optimization using fine-grained rewards is essential for grounding high-level cognitive analysis in physical reality.

Perception-Reasoning Trade-off. We observe a slight regression in atomic \mathcal{L}_1 Perception tasks at Stage 4 (65.19% \rightarrow 63.64%). This indicates a subtle trade-off: as the model optimizes for complex, multi-hop reasoning rewards (which prioritize the final logical conclusion), it may slightly relax its focus on low-level extraction tasks. However, this minor cost is outweighed by the massive gains in reasoning reliability. Notably, the *Count Objects* task, typically a weakness for LALMs, achieves a respectable 60% accuracy, demonstrating that the model retains strong numeracy even after RL alignment.

6. Conclusion

To bridge the spatial gap in LALMs, we proposed TWNM, a unified framework grounded in our Three-Layer ASA Taxonomy. By integrating a disentangled spatial encoder with a Dense Hybrid Projector and a progressive curriculum culminating in Soft Adaptive Policy Optimization (SAPO), TWNM achieves robust spatial reasoning capabilities. Evaluation on our benchmark demonstrates significant gains over state-of-the-art baselines, particularly in high-level abductive reasoning and real-world generalization (via Sim-to-Real mixing). While challenges remain in fine-grained numeracy and full end-to-end real-world adaptation, our work establishes a critical foundation for physically grounded audio intelligence. Future research will target large-scale embodied data collection to further close the reality gap.

References

- Agostinelli, A., Denk, T. I., Borsos, Z., Engel, J., Verzetti, M., Caillon, A., Huang, Q., Jansen, A., Roberts, A., Tagliasacchi, M., Sharifi, M., Zeghidour, N., and Frank, C. MusiCm: Generating music from text, 2023. URL <https://arxiv.org/abs/2301.11325>.
- Bregman, A. S. *Auditory Scene Analysis: The Perceptual Organization of Sound*. The MIT Press, 05 1990. ISBN 9780262269209. doi: 10.7551/mitpress/1486.001.0001. URL <https://doi.org/10.7551/mitpress/1486.001.0001>.
- Chu, Y., Xu, J., Yang, Q., Wei, H., Wei, X., Guo, Z., Leng, Y., Lv, Y., He, J., Lin, J., Zhou, C., and Zhou, J. Qwen2-audio technical report. *arXiv preprint arXiv:2407.10759*, 2024. URL <https://arxiv.org/abs/2407.10759>.
- Devnani, B., Seto, S., Aldeneh, Z., Toso, A., Menyaylenko, E., Theobald, B.-J., Sheaffer, J., and Sarabia, M. Learning spatially-aware language and audio embeddings, 2024. URL <https://arxiv.org/abs/2409.11369>.
- Drossos, K., Lipping, S., and Virtanen, T. Clotho: An audio captioning dataset, 2019a. URL <https://arxiv.org/abs/1910.09387>.
- Drossos, K., Lipping, S., and Virtanen, T. Clotho: An audio captioning dataset, 2019b. URL <https://arxiv.org/abs/1910.09387>.
- Du, J., Wu, D., Wu, X., and Qu, T. An envelope separation aided multi-task learning model for blind source counting and localization. In *IEEE International Conference on Acoustics, Speech and Signal Processing (ICASSP)*, 2026. Accepted.
- Fedus, W., Zoph, B., and Shazeer, N. Switch transformers: Scaling to trillion parameter models with simple and efficient sparsity, 2022. URL <https://arxiv.org/abs/2101.03961>.
- Fonseca, E., Favory, X., Pons, J., Font, F., and Serra, X. Fsd50k: An open dataset of human-labeled sound events, 2022. URL <https://arxiv.org/abs/2010.00475>.
- Gao, C., Zheng, C., Chen, X.-H., Dang, K., Liu, S., Yu, B., Yang, A., Bai, S., Zhou, J., and Lin, J. Soft adaptive policy optimization, 2025. URL <https://arxiv.org/abs/2511.20347>.
- Goel, A., Ghosh, S., Kim, J., Kumar, S., Kong, Z., Gil Lee, S., Yang, C.-H. H., Duraiswami, R., Manocha, D., Valle, R., and Catanzaro, B. Audio flamingo 3: Advancing audio intelligence with fully open large audio language models, 2025. URL <https://arxiv.org/abs/2507.08128>.
- Hu, J., Cao, Y., Wu, M., Kong, Q., Yang, F., Plumbley, M. D., and Yang, J. A track-wise ensemble event independent network for polyphonic sound event localization and detection, 2022. URL <https://arxiv.org/abs/2203.10228>.
- Huang, R., Li, M., Yang, D., Shi, J., Chang, X., Ye, Z., Wu, Y., Hong, Z., Huang, J., Liu, J., Ren, Y., Zhao, Z., and Watanabe, S. Audiogpt: Understanding and generating speech, music, sound, and talking head, 2023. URL <https://arxiv.org/abs/2304.12995>.
- Koizumi, Y., Zen, H., Karita, S., Ding, Y., Yatabe, K., Morioka, N., Bacchiani, M., Zhang, Y., Han, W., and Bapna, A. Libritts-r: A restored multi-speaker text-to-speech corpus, 2023. URL <https://arxiv.org/abs/2305.18802>.
- Lepikhin, D., Lee, H., Xu, Y., Chen, D., Firat, O., Huang, Y., Krikun, M., Shazeer, N., and Chen, Z. Gshard: Scaling giant models with conditional computation and automatic sharding, 2020. URL <https://arxiv.org/abs/2006.16668>.
- Manco, I., Weck, B., Doh, S., Won, M., Zhang, Y., Bogdanov, D., Wu, Y., Chen, K., Tovstogan, P., Benetos, E., Quinton, E., Fazekas, G., and Nam, J. The song describer dataset: a corpus of audio captions for music-and-language evaluation, 2023. URL <https://arxiv.org/abs/2311.10057>.
- Rafaely, B. *Fundamentals of spherical array processing*, volume 8. Springer, 2015.
- Rajbhandari, S., Rasley, J., Ruwase, O., and He, Y. Zero: Memory optimizations toward training trillion parameter models. *arXiv preprint arXiv:1910.02054*, 2020.
- Scheibler, R., Bezzam, E., and Dokmanić, I. Pyroomacoustics: A python package for audio room simulations and array processing algorithms. *arXiv preprint arXiv:1710.04196*, 2017. URL <https://arxiv.org/abs/1710.04196>.
- Shao, Z., Wang, P., Zhu, Q., Xu, R., Song, J., Bi, X., Zhang, H., Zhang, M., Li, Y. K., Wu, Y., and Guo, D. Deepseekmath: Pushing the limits of mathematical reasoning in open language models, 2024. URL <https://arxiv.org/abs/2402.03300>.
- Shimada, K., Koyama, Y., Takahashi, N., Takahashi, S., and Mitsufuji, Y. Accdoa: Activity-coupled cartesian direction of arrival representation for sound event localization and detection, 2021. URL <https://arxiv.org/abs/2010.15306>.

Shimada, K., Koyama, Y., Takahashi, S., Takahashi, N., Tsunoo, E., and Mitsufuji, Y. Multi-acccdo: Localizing and detecting overlapping sounds from the same class with auxiliary duplicating permutation invariant training, 2022. URL <https://arxiv.org/abs/2110.07124>.

Shimada, K., Politis, A., Sudarsanam, P., Krause, D., Uchida, K., Adavanne, S., Hakala, A., Koyama, Y., Takahashi, N., Takahashi, S., Virtanen, T., and Mitsufuji, Y. Starss23: An audio-visual dataset of spatial recordings of real scenes with spatiotemporal annotations of sound events, 2023. URL <https://arxiv.org/abs/2306.09126>.

Tang, C., Yu, W., Sun, G., Chen, X., Tan, T., Li, W., Lu, L., Ma, Z., and Zhang, C. Salmonn: Towards generic hearing abilities for large language models, 2024. URL <https://arxiv.org/abs/2310.13289>.

Yang, Q., Xu, J., Liu, W., Chu, Y., Jiang, Z., Zhou, X., Leng, Y., Lv, Y., Zhao, Z., Zhou, C., and Zhou, J. Air-bench: Benchmarking large audio-language models via generative comprehension, 2024. URL <https://arxiv.org/abs/2402.07729>.

You, Y., Qian, Y., Qu, T., Wang, B., and Lv, X. Spherical harmonic beamforming based ambisonics encoding and upscaling method for smartphone microphone array. In *Audio Engineering Society Convention 158*. Audio Engineering Society, 2025.

Zheng, Z., Peng, P., Ma, Z., Chen, X., Choi, E., and Harwath, D. Bat: Learning to reason about spatial sounds with large language models, 2025. URL <https://arxiv.org/abs/2402.01591>.

Appendix

A. Data Simulation Details

To ensure the diversity and physical realism of our training data, we implemented a comprehensive simulation pipeline governed by the following parameters.

Room Acoustics and Geometry. We generate Room Impulse Responses (RIRs) using the `pyroomacoustics` simulator (Scheibler et al., 2017). Rooms are modeled as shoebox shapes with dimensions sampled uniformly from three categories:

- **Small:** $x \in [3, 5]$ m, $y \in [4, 6]$ m, $z \in [2.5, 3.5]$ m
- **Medium:** $x \in [8, 12]$ m, $y \in [10, 15]$ m, $z \in [3, 5]$ m
- **Large:** $x \in [20, 30]$ m, $y \in [25, 35]$ m, $z \in [10, 15]$ m

Wall absorption coefficients $\alpha_{\text{abs}} \in [0, 1]$ are sampled to simulate varying Reverberation Times (RT60):

- **High Reverberation (Reflective):** $\alpha_{\text{abs}} \in [0.05, 0.25]$
- **Medium Reverberation:** $\alpha_{\text{abs}} \in [0.25, 0.5]$
- **Low Reverberation (Absorptive):** $\alpha_{\text{abs}} \in [0.5, 0.95]$

For each room, we randomly place one receiver and 30 candidate source positions.

Source Material and Scene Synthesis. Dry clips are convolved with the generated BRIRs, scaled by a random gain, and summed to create the final mixture. This pipeline ensures precise ground-truth labels for \mathcal{L}_1 (location, class) and \mathcal{L}_2 (spatial relations) tasks.

Data Formats. The training data evolves across stages:

- **SFT Data:** The initial stage employs open-ended QA pairs to align the Feature Projector with the LLM. The subsequent SFT stage introduces Chain-of-Thought (CoT) formatting (using `<think>` and `<answer>` tags) to prime the model for reasoning.
- **RL Benchmark:** A held-out set of multiple-choice questions designed to probe specific spatial competencies, serving as the environment for reinforcement learning.

B. Training Implementation Details

Hyperparameters. We utilize the AdamW optimizer across all training stages. The detailed hyperparameter configuration for each stage of our progressive curriculum is provided in Table 4.

Hyperparameter	Stage 2	Stage 3	Stage 4
Learning Rate	1×10^{-4}	5×10^{-5}	1×10^{-6}
Batch Size (Global)	128	128	64
Epochs	2	3	1
Warmup Ratio	0.03	0.03	0.1
Gradient Clipping	1.0	1.0	1.0
LoRA Rank (r)	N/A	8	8
LoRA Alpha (α)	N/A	32	32
Optimizer	AdamW	AdamW	AdamW

Table 4. Hyperparameter settings for different training stages.

SAPO Setting. For each query, we generate $G = 8$ roll-outs and compute advantages using a fine-grained, weighted reward function:

$$R(y) = 2.0r_{\text{fmt}} + 1.0r_{\text{val}} + 3.0r_{\text{cor}} + 0.5r_{\text{len}} + 0.5r_{\text{evd}} + 0.2r_{\text{ref}} \quad (10)$$

The components are defined as follows:

- (1) r_{fmt} ensures strict adherence to the XML-style reasoning structure;
- (2) r_{val} validates that the output is a legitimate option (A–D);
- (3) r_{cor} rewards prediction accuracy against the ground truth;
- (4) r_{len} penalizes reasoning chains that deviate from an optimal length window (40–400 characters) to discourage verbosity;
- (5) r_{evd} incentivizes grounding by detecting auditory keywords (e.g., “sound”, “hear”); and
- (6) r_{ref} acts as a negative constraint, penalizing hallucinations where the model references the text prompt description instead of the audio.

To mitigate reward hacking and prevent KL explosion, we implement an adaptive KL Penalty mechanism. The penalty coefficient β is dynamically scaled based on the moving average of the KL divergence between the current policy and the reference model: β increases if the divergence exceeds a target threshold and decreases otherwise. Furthermore, we initialize the Stage 4 LoRA adapters with a Gaussian distribution rather than zero to ensure stable gradient flow at the onset of reinforcement learning.

System Configuration. All experiments were conducted on a cluster of 6 NVIDIA RTX 5090 GPUs (32 GB VRAM each). We leverage `torchrun` for distributed training and utilize the DeepSpeed ZeRO Stage 2 strategy (Rajbhandari et al., 2020) with CPU offloading to maximize memory efficiency. The framework is implemented using PyTorch and the Hugging Face Transformers library.

C. Prompt for Benchmark Generation

Prompt (for generating open-ended spatial QA)

You are a top-tier AI course designer preparing graduation exam questions for an advanced spatial audio model. This model has already mastered the basics of recognizing sound content (semantic), localizing sources (localization), perceiving the environment (acoustics), and counting (count). Your task: given a `<scene_description>`, design 1–2 **open-ended**, complex questions that require integrating multiple abilities, and provide detailed, fluent, high-quality answers.

[Design Principles]

- **Reject simplicity:** do not ask “Where is the dog?”; instead ask “What is the main activity in the scene, and where does it occur relative to me in space?”
- **Encourage reasoning:** propose questions that require inference from multiple cues. For example: “Based on the room’s reverberation and the sounds inside, what is the most plausible type of place?”
- **Simulate dialogue:** both questions and answers should read like a natural conversation between humans.

[Example] `<scene_description>`

Indoors with slight reverberation, two sounds are audible. One is keyboard typing from straight ahead at a close distance. The other is birdsong coming from outside the window, located up-right and farther away.

`</scene_description>`

`<generated_data>`

```
[
  {
    "instruction": "Based on what you hear, can you infer where I might be and what I'm doing?",
    "answer": "It sounds like you're likely in a room—perhaps an office or at home. The clear, nearby keyboard typing suggests you're working or studying on a computer. Meanwhile, the birdsong from outside implies it's likely daytime and that you're close to a window."
  }
]
```

`</generated_data>`

[Formal Task] `<scene_description>`

`{{ insert RTSD here }}`

`</scene_description>`

`<generated_data>`

`</generated_data>`

D. Case Study

To further illustrate the reasoning ability of our model, we present a representative case study drawn from the evaluation set. The task requires the model to infer the most plausible explanation of an acoustic scene based on the perceived spatialized audio.

Table 5. **Overview of the TWNM Spatial Reasoning Benchmark.** The benchmark covers three cognitive levels (\mathcal{L}_1 – \mathcal{L}_3), derived from the ASA framework. Tasks are generated via rule-based prompts ensuring strict ground-truth alignment.

Level	Task Family	Specific Tasks	Example Question Template
\mathcal{L}_1	Numeracy	Count Objects	“How many independent sound sources are audible in the clip?”
	Semantics	Identify Event Class	“Which of the following sounds is present in the audio?”
		Identify Speech Transcript	“What specific phrase was spoken in the audio?”
	Spatial Physics	Localize Azimuth	“What is the horizontal direction (azimuth) of the [Event X]?”
Localize Elevation		“Is the [Event X] coming from above, below, or eye-level?”	
Estimate Distance		“Approximately how many meters away is the [Event X]?”	
Environment Acoustics		“Which description best matches the room size and reverberation?”	
\mathcal{L}_2	Binding	Attribute Verification	“Which statement accurately describes the content, location, and distance?”
	Retrieval	Query Location given ID	“Where is the [Event X] located?”
		Query ID given Location	“What sound is coming from the rear-left, approximately 4m away?”
	Comparison	Relative Distance	“Which sound is closer to the listener, [Event A] or [Event B]?”
Relative Direction		“Is [Event A] positioned to the left or right of [Event B]?”	
\mathcal{L}_3	Abduction	Scene Abduction	“Based on the sounds and acoustics, what is the most likely scene?”
		Causal Intent	“What activity or intent is best implied by the sequence of sounds?”
	Counterfactual	Rotate Observer (180°)	“If you turn around 180°, where would [Event X] be located now?”
		Source Removal	“If the sound of [Event X] is removed, which statement remains true?”
Logic & Physics	Multi-hop Query	“Identify the farthest sound source and state its direction.”	
	Physical Consistency	“Which statement is physically impossible given the room dimensions?”	

Ground Truth (Reference)

Scene Description:

- **Scene type:** Mixed, single sound source
- **Sound event:** Respiratory sound (breathing)
- **Azimuth:** 317°, **Elevation:** -13°, **Distance:** 17.4 m
- **Room acoustics:** Anechoic, absorption coefficient ≈ 0.99 , RT60 = 0.0 s

Correct Answer:

A. The listener may be using headphones to hear a specially recorded or processed audio, in which a breathing sound is precisely placed at a specific position in the sound field.

Question

Task: Based on the audio you hear, which of the following explanations is the most reasonable for this scene?

- A. The listener may be using headphones to hear a specially recorded or processed audio, in which a breathing sound is precisely placed at a specific position in the sound field.
- B. In a wide-open space, someone is breathing about 17 meters away from the listener, and the openness of the space makes the sound unusually clear.
- C. The listener is in a completely silent room, and due to over-concentration, hallucinates the distant sound of breathing.
- D. This is a live recording in a large concert hall, where a breathing sound from an audience member was mistakenly amplified during post-production.

Model Output (verbatim)

|<think>| The core of the question is to infer the most reasonable scene based on the heard sound. First, I analyze the key sound elements in the audio. I heard a clear breathing sound, coming from my front-left, about 17 meters away. The sound is very clear, almost without echo, which indicates I am in an open environment, such as a large space. The sound position is very precise, at azimuth 313 degrees and elevation 1 degree, which shows that the sound source is fixed rather than moving randomly. Based on these observations, I evaluate each option:

- Option A states that the breathing sound was placed at a specific position. This matches exactly with the sound location I heard (azimuth 313 degrees). A processed audio, where a sound is placed at a specific position in the recording, is entirely possible.
- Option B describes a wide-open space with someone breathing. This contradicts the clear, echo-free sound characteristics. A wide-open space would produce noticeable reverberation.
- Option C suggests that the sound is a hallucination from silence. This is clearly wrong because I distinctly heard a breathing sound.
- Option D suggests a concert hall live recording where the breathing was over-amplified. However, a concert hall should have noticeable reverberation, which is absent here, so D is not reasonable.

In summary, Option A best fits the sound characteristics: a clear, precisely located breathing sound placed in a large space.|</think>|

According to the audio analysis, the sound comes from a precise location in a nearly echo-free large space, indicating that it is likely a processed audio rather than a real-world event.

|<answer>| A |</answer>|